S.A.B.R.E - Smart Assessing Breaker for Residential Environments

Carter Harman, Emmanuel Lopez, David Durosinmi, Eliezer Urdaneta

Dept. of Electrical Engineering and Computer Science, University of Central Florida, Orlando, Florida, 32816

***Abstract* — Modern circuit breakers have been widely adopted into all residential buildings over the past century, so much so that to comply with the National Electric Code (NEC), all modern residential buildings are required to have them installed. These breakers utilize principles of electromagnetism to trip mechanically flip and halt the flow of current along a branch within a residential building. This paper's primary focus is on the modernization of the simple circuit breaker by introducing an approach involving removing the mechanical aspect of the conventional circuit breaker and replacing it entirely with electrical components granting the user access to internet-of-things (IoT) by allowing them to view and collect real-time and past data from anywhere in the world, while maintaining the efficiency and reliability of what makes residential circuit breakers so abundant.**

***Index Terms* — Electrical safety, fault detection, Internet of Things, power electronics, printed circuits boards, real-time systems, web services.**

I. Introduction

Modern circuit breakers have been something of a staple within any residential building constructed within the past century. The circuit breakers seen in homes today are seen composed of thermal-magnetic bimetal strips that are used as the conductor to allow current to flow from the main power grid throughout a branched subsection of a building. Breakers are specified with certain thresholds in terms or amperage and temperature, and when exceeding these thresholds, causes the bimetal strips to breakaway, or "trip", and halt the flow of current being delivered along its branch. While reliable, standard circuit breakers have managed to maintain this design principal over the last 50 years. The project's primary focus is on taking the efficiency and reliability of circuit breakers and bringing them into the modern age by utilizing sensors, solid-state halting, wireless data transmitting and monitoring, and custom parameter setting.

This smart, single-phase, circuit breaker looks to act as a low power reference to be expanded on for a future full scale smart breaker that can provide real-time monitoring, wireless remote control from outside of the home, and management of energy consumption in a residential building. This is achieved by introducing a microcontroller capable of reading and transmitting incoming data along the signal line to a remote server, in which it can be accessed from a web browser client to monitor and control the incoming signal. In addition, the inclusion of a solid-state trip mechanism allows for a faster trip time while offering a more robust implementation as compared to the mechanical switching seen in circuit breakers of today.

II. System Specifications

Due to safety concerns in relation to utilizing standard mains voltage (120V/240V) in this project, the team was advised to produce a scaled down iteration that operated at 24V with a maximum current of 5 amperes (A).

TABLE I
SYSTEM SPECIFICATIONS

Specification	Value	Tolerance
Operating Voltage	24 VAC	±10%
Max. Rated Current	5 A	±5%
Max. Rated Temp.	100 C °	-
Trip Response Time	<= 5ms	±5%
Wireless Trip Instr.	< 3s	±5%
Power Consumption	< 10W	±10%
Continuous Load Rating	95% of defined max	-
Dimensions (H x W x D)	75 x 40 x 80mm	±1%

Table I showcases the most penitent system specifications for the S.A.B.R.E. Smart Breaker. Trip response time refers to the time it takes for the breaker to halt current flow once the value of current has exceeded the user defined max. Wireless trip instruction is in regard to the amount of time it takes for the breaker to manually trip once a user has requested to toggle the breaker remotely from the web client. Continuous load rating specifies the value at which continuous operation of the breaker does not lead to any trip condition being met.

III. SYSTEM HARDWARE

The system is most effectively described through a detailed explanation of individual components and how they interact with one another to make up the physical aspects of the S.A.B.R.E. Smart Circuit Breaker. The following details exactly that by giving an overview of each component, and their role in making up of the overall system.

A. Microcontroller Unit

At the center of the S.A.B.R.E Smart Breaker is the ESP32-WROOM-32 microcontroller unit. The ESP32 boasts a dual-core processor capable of operating at clock speeds upwards of 240 MHz. Its System On Chip (Soc) design allows for features such as an onboard digital-to-analog converter, physical antenna, and Wi-Fi connectivity allows for rich peripheral support packed tightly into a small form factor. In addition, the chip comes equipped with 448KB of ROM, 520KB of SRAM, and 4MB of flash memory [1], allowing for more than enough overhead in terms of memory capacities. The ESP32 was programmed with C++ with the Platform IO IDE along with the vast ecosystem of opensource Arduino libraries.

B. Trip Mechanism — Solid-State Relay

The S.A.B.R.E Smart Breaker employs a solid-state relay, specifically the Toshiba TLP3547, to manage the "tripping" function, which interrupts the current flow. This relay can safely handle a maximum of 5A of root-mean-squared (RMS) current at voltages up to 60 volts RMS. The relay's operation is governed by a photo MOSFET that is optically linked to an infrared LED. A minimal current signal is sufficient to activate the internal infrared LED, which in turn toggles the continuity of the MOSFET network [2].

C. Current Measuring — Hall-Effect Sensor

To measure the amperage of the signal delivered to the load, the smart breaker utilizes a Hall-Effect Sensor that is capable of producing an analog voltage signal proportional to the current flowing through it. Specifically,

$$V = R_h \left(\frac{I}{t} \cdot B\right) \quad (1)$$

Where V is the Hall Voltage, Rh is the Hall-Effect coefficient, I is the current, t is a sensor constant, and B is the magnetic flux density in Teslas [3]. The Hall Voltage is then internally biased and amplified through an Op-Amp to provide a usable analog signal. This signal is then able to be read from the ESP32's onboard ADC, and using specified equations can be converted back into the current representation. The Hall-Effect sensor selected to be utilized is the ACS712-20A due to its small form-factor, relatively high maximum current rating, and a reasonable gain in respect to the analog voltage produced. The ESP32's onboard ADC is notoriously noisy and inaccurate nearing its minimum and maximum values. However, the ACS712-20A's idle state, when no current is passing through, is centered at half of its supply voltage. With a supply voltage of 5A, this means that the analog voltage produced will swing around this midpoint value, depending on the polarity of the current, instead of linearly increasing from 0V upwards as the current flowing across it increases [4].

D. Temperature Monitoring — Thermistor IC

To perform temperature monitoring for safety, the S.A.B.R.E Smart Breaker has employed the use of a small Thermistor IC right along the main signal trace. The IC utilized is the MCP9700, providing a maximum operating range of -40°C to +125°C with an accuracy of ±2° Celsius between temperatures of 0° C - 70° C [5]. This IC works in a similar fashion to the ACS712-20A mentioned previously, in which it produces an analog voltage signal centered around the supply voltage at room temperature, and shifts accordingly with the change in measured temperature.

E. Local Interaction — Liquid Crystal Display (LCD)

Due to its "smart" functionality, the S.A.B.R.E Smart Breaker necessitates local provisioning during the initial setup. Specifically, the breaker requires the input of Wi-Fi and account credentials to properly link and view transmitted data wirelessly. To facilitate this, the team designed a custom PCB that communicates with the display's integrated ST7789 controller via the SPI protocol. Beyond handling the initial setup and credential prompts, the display also provides a local view of the measurements taking place with a modern UI that aligns with the remote client dashboard. To provide the same local interaction of that of a conventional circuit breaker, the S.A.B.R.E. Smart Breaker provides a switch to physically toggle the flow of current locally at the breaker itself.

F. Low-Power Supply Regulation

Considering that conventional circuit breakers are not equipped with internal electronics and thus do not require external power sources like batteries, the S.A.B.R.E. Smart Breaker mimics this approach by utilizing the main signal line to provide a constant power source to its internal electronics without the need for an external supply. Because the main load line carries an AC signal, a full-bridge rectifier (FBR) is paramount to convert the AC signal to a DC signal. This is done in tandem with a switching-buck regulator to lower the output voltage to a suitable 5V, capable of safely powering the internal electronics. This regulating circuit is centered around the LM2576-HV IC, which can take a DC voltage input between 7V and 60V and effectively step it down to the desired 5V DC output. Additionally, this setup ensures high conversion efficiency and minimizes voltage ripple, which is crucial for maintaining stable operation when the ESP32 draws sudden current spikes during Wi-Fi data transmission.

G. Mains Supply

Due to safety concerns mentioned previously, the project scope was scaled back to have the breaker implementation only operate at a 120 Volt-Amps (VA), a significant reduction from the 1650 VA typical of low-end mechanical breakers. To support this, the team utilized a 120 VA transformer capable of delivering 24 V_{RMS} at 5 A. This transformer allows the S.A.B.R.E Smart Breaker to be powered via a standard mains outlet while maintain safe levels for demonstration.

H. Hardware Block Diagram

Now that individual components have been highlighted, the hardware interactions that facilitate this process can be detailed. Each of the major components is presented here to showcase the general interaction between the respective peripherals.

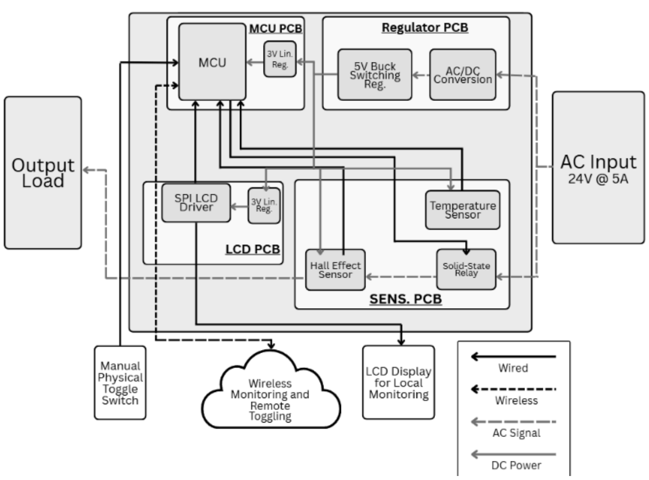

Fig. 1. Block diagram all major component interactions on their respective PCBs.

The block diagram illustrates the organization of components across four printed circuit boards (PCBs), categorized by their interactions amongst each other. The smart breaker comprises several key elements: the MCU board, which facilitates the transmission of inputs and outputs among the boards; the regulator board, equipped with the essential hardware to generate a power source for all internal electronics; an LCD board that interfaces with the embedded TFT chip of the LCD via SPI; and the sensor PCB, which routes and processes the main AC signal line and captures data from the associated sensors.

IV. SYSTEM SOFTWARE

A. Firmware

As mentioned previously, the firmware written for the ESP32 was written in C++ and utilizes a lot of abstracted classes and methods provided by the extensive Arduino ecosystem. The main C++ is composed of strictly calling functions defined in additional header files, allowing for the startup and main loop to be modular and easily understandable from an outsider's perspective.

```
if(!THRESHOLDS_PROVISIONED)
    promptUserForThresholds();
if(!WIFI_CREDS)
    promptWIFICredentials;
if(!CONNECTED_TO_WIFI)
    connectToWIFI();
if(!CONNECTED_TO_REMOTE)
    connectToServer();
if(CONNECTED_TO_WIFI && CONNECTED_TO_REMOTE && !ACCOUNT_CREDS_ENTERED)
{
    if(SAVED_ACCOUNT_CREDS)
        checkPrevSavedCredsFromMem();
    else
        promptUserCredentials();
}

if(ACCOUNT_CREDS_ENTERED && !REGISTERED_DEVICE)
    linkDeviceToAccount();
else if(ACCOUNT_CREDS_ENTERED && REGISTERED_DEVICE)
{
    if(!UI_SETUP)
        drawInitialUI();
    else if(!OFFSET_VOLT_SET)
        setOffsetVoltage();
    else
    {
        float sum_of_squares = (offset_votlage);
        rms_struct_t rms_struct = calculateRMSValues(sum_of_squares);
        drawUI(rms_struct.current);
        drawUI(rms_struct.temperature);
        pollCommandFromServer();
        remoteTransmitFunction(rms_struct, MAX_CURRENT, MAX_TEMP, TRIGGERED);
    }
}
```

Fig. 2. Main running program loop including startup sequence and measurement stage

Fig. 2 shows an abridged showcase of the main loop function. Upon a reset, the device runs through its startup sequence, prompting the user to set parameters for current and temperature thresholds, Wi-Fi credentials, and account credentials. If these parameters have been set on a prior startup, this sequence can be bypassed to allow the user to avoid having to set these upon every reset. Once this sequence has completed, the device will draw the UI elements along the LCD, take an initial offset measurement to be properly calibrated with respects to the idle state with no current passing, and then allows current to flow and begins taking measurements.

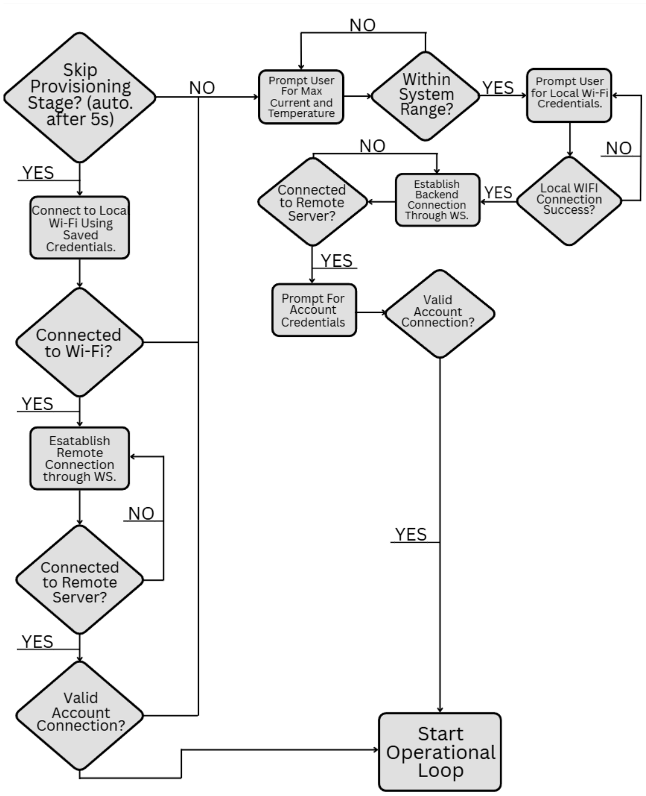

Fig. 3. Software flowchart of the S.A.B.R.E start up sequence.

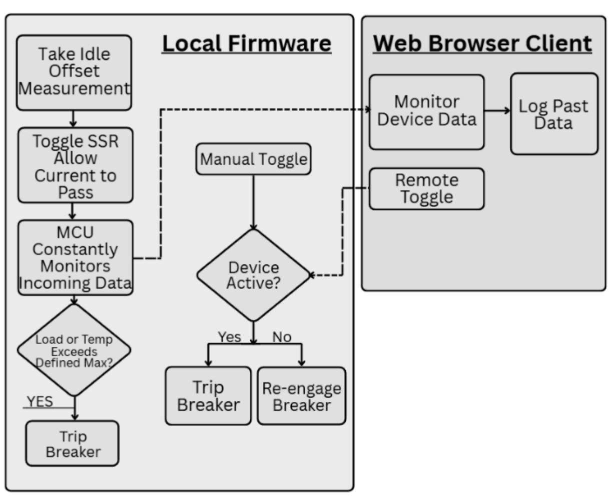

Fig. 4. Software flowchart of the main S.A.B.R.E Operational Loop.

Due to the dual-core architecture of the ESP32, all Wi-Fi based communication is segmented (change this) to execute independently on its own core, as to not bog down or interrupt any of the capturing and computation of measurements occurring locally which utilizes the other processor. In addition to this, the switch responsible for locally tripping the breaker is tied to the interrupt handler on the ESP32, as to avoid constantly polling this pin and so that no matter where in the execution cycle the program might be at the breaker will be sure to instantly toggle on or off.

B. Measurements

Measuring a DC signal through the Hall-Effect sensor is trivial, just capture the drift in voltage relative to the initial offset that was captured, and then apply the conversion specified in the datasheet to calculate the DC signal across the sensor. The ESP32's high sampling frequency of its ADC also allows for accurate measurements of specific points in time along an AC waveform, making it again trivial to capture the fluctuation of the magnitude of a given signal. However, the AC voltage rating of the main electrical grid is expressed in terms of its RMS voltage, as this provides an accurate representation of the effective voltage needed to deliver the same power to a load as its DC equivalent. This principle extends to the current generated by the voltage waveform, which is why conventional circuit breakers are also rated based on the RMS value of the current. Consequently, to align with standard circuit breaker functionality, the S.A.B.R.E. Smart Breaker must also be rated in terms of the current's RMS value. Due to this fact, calculating individual current values at different points along the waveform will yield results differing from those of a conventional breaker, as the calculated current will fluctuate depending on the sampling point along the waveform, rather than maintaining a constant value as would be observed with an AC signal measured by a digital multi-meter (DMM). Because of this, the S.A.B.R.E. Smart Breaker needs to calculate the RMS equivalent of the AC waveform. This is done in accordance with the following equation,

$$V_{RMS} = \sqrt{\frac{1}{T}\int v(t)^2 dt} \quad (2)$$

Which states that the RMS voltage is equal to the square root average of the area under the curve of the squared waveform function [6]. In practice this equation is implemented as

$$V_{RMS} = \sqrt{\frac{1}{N}\sum_{n=1}^{N} V_n^2} \quad (3)$$

Where N corresponds to the number of individual voltage samples taken along a waveform for a given RMS measurement. N is chosen in conjunction with a specified sampling frequency to properly sample along a window that corresponds to M full sinusoidal cycles, so as to properly capture the necessary information required to compute the RMS voltage.

V. WEB APPLICATION

The Webapp serves as a remote client that communicates with the ESP32 via a backend server through a WebSocket connection. The communication starts from the ESP32, then it sends requests to the remote node server, and the response is reflected onto the web application.

A. Web Application Contents

The remote Webapp features a home page that provides essential information on setting up and registering a user account, along with general details about the S.A.B.R.E. Smart Breaker. Additionally, it offers access to pages for logging into an existing account or registering as a new user. Upon logging in, users will be welcomed by the main dashboard, which displays all devices registered to their account. The left side of the screen features an interactive sidebar that facilitates navigation to other pages, including user settings and a page for reviewing previously logged data.

The dashboard page features a comprehensive overview of each listed device, presenting essential details such as the device ID, its online status, the values currently being monitored, and a remote toggle button for the breaker operation. Additionally, the interface includes visual representations of the temperature and current levels, displayed as progress rings and bars that indicate the percentage of their maximum values.

B. Backend Communication Protocols

Two complimentary protocols are used to facilitate communication between the ESP32 and the server. WebSockets provide full-duplex, real-time streaming data from the MCU to a user's dashboard, while the REST API is utilized for conventional create, read, update, and delete (CRUD) operations. In particular, the ESP32 ensures that data is sent to the appropriate authorized session by posting data to specific WebSocket connections that correspond by a user ID and a registered device ID. The WebSocket connection for sensor monitoring is essential to the system's real-time monitoring capacity since it avoids away with the recurrent handshake overhead of HTTP and REST API polling.

C. Technology Stack

The S.A.B.R.E. web application features a full stack architecture, utilizing a React frontend with TypeScript to ensure type safety and enhance UI component reusability across various pages. The backend is developed using Node.js with Express, serving as middleware to provide REST APIs for essential functions such as user login and authentication. Additionally, the backend server is where the WebSocket connections are made between user clients and their registered devices. For long-term persistent data storage, the application employs MongoDB, a NoSQL database adept at handling unstructured high-volume data, continuous IoT sensor logs, device configurations, and user information and settings.

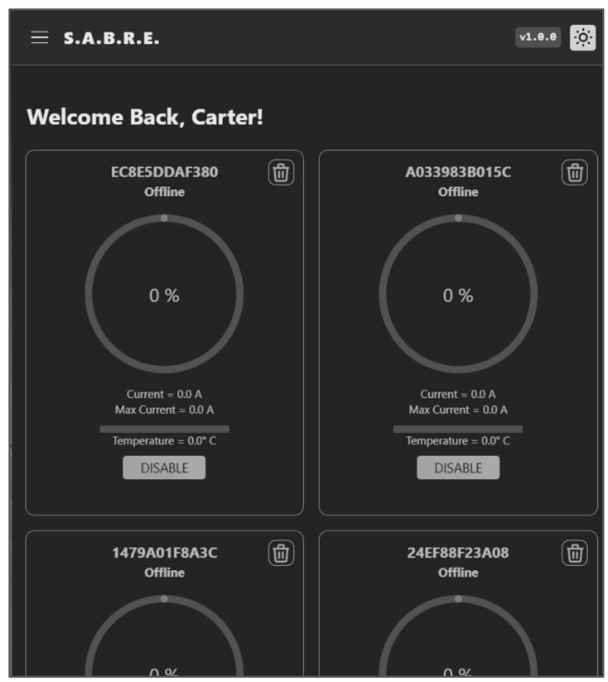

Fig. 5. Showcase of UI on mobile for a user's dashboard page.

VI. SAFETY REQUIREMENTS

Due to safety concerns for the team as university students and due to our inexperience with high level voltages, the project was restricted to 24 V at 5 A to greatly reduce risk of injury, however, IEEE and NESC standards were still implemented within the project, though at a reduced scale.

A. Shock Safety

The first concern for safety within the SABRE prototype was the risk of being electrocuted. According to IEEE for voltages running at 120 V-240 V, currents as low as 9 mA can cause involuntary muscle contraction or the inability to let go of a conductor [7]. In order to ensure maximum safety, all connections will use safe wiring practices, insulation will be verified, and all exposed conductors will be rated for the voltage and current used. Proper grounding procedures, protective covers, and documented wiring and protective-device standards will be followed.

B. Low-Voltage Circuit Breaker Standards for Trip Systems

IEEE C37.17-2022 [8] defines how a trip system inside a low-voltage circuit breaker must operate, perform, and protect electrical equipment under 1 kV. To classify as a protective system, the device must fulfill these basic protection requirements: Overload protection, Instantaneous protection, Ground-fault protection functions, Environmental performance, Reset and Reclose characteristics, Power supply Requirements, Display and indication requirements, and Data and communication requirements.

C. Transformer Safety

IEC 61558 [9] is an essential safety standard to the SABRE smart breaker as the first subsystem that the power must go through is the transformer. To safely comply with standards, the transformer must first meet insulation requirements protecting individuals from electric shock. Then it must clear clearance and creepage distance requirements to remove the possibility of arcing between two conductive terminals. Lastly, the thermal and electrical safety requirements in which the support structure for the windings of the transformer play a crucial role in the operation and safety of the component. Terminals must be adequately marked within either the chassis or the datasheet of our design. Lastly, the transformer output voltage must be tested under no load and with an applied load to gauge the current drawn from the applied load.

D. PCB Design Standards

IPC-2221 [10] standard is a generic design guideline outlining the proper assembly of printed circuit boards regarding conductor spacing, trace width, clearance, creepage, material selection, mounting methods, and general layout principles. Specific spacing within the standards can be found depending on peak voltage potentials between conductors giving accurate data on the minimum amount of internal and external spacing within conductors. Most importantly within this standard includes the following equation that determines the thickness of the conductive traces within the PCBs:

$$I = k \cdot \Delta T^{0.44} \cdot A^{0.725} \quad (4)$$

Generally, the thickness of the traces within PCBs were only determined on ease of accessibility, however, within this PCB, sizing mattered due to the large amount of current being drawn. Anything smaller would destroy the trace causing potential hazards and anything larger would impede our sizing requirements.

VII. TESTING AND VALIDATION

The S.A.B.R.E. smart breaker system's strong performance depends on a thorough testing and validation approach that covers both software and hardware implementation.

To simulate a 25VAC signal, the TR100VA001 was used for high performance testing. To confirm its output delivery rating, a resistive load of 12 **Ω**, rated for a total of 100 watts was placed in parallel with the power source to measure its effectiveness.

The TLP3547 SSR was validated by confirming complete isolation between the LED driven control side and the primary MOSFET signal side to ensure no measurable leakage or continuity to prevent ground loops, regardless of the state the relay was in. Once confirmed, a low-level voltage DC conduction test was performed using a 9V battery placed across the signal terminals and controlled through a 5V signal sourced from a generic microcontroller. This verified correct turn on thresholds for current driven LED for the optocoupler inside and gave a rough real-world measurement to showcase the minimum power loss over the internal MOSFET array. Following this, the SSR performed through a high voltage AC conductivity test by applying the secondary side of the transformer to the input terminals to assess proper operation during the intended scenario, and to confirm minimal to no waveform distortion from the internal solid-state components. To ensure effective performance under continuous load, the relay was subjected to 2.5A of alternating current by introducing the previously mentioned 12Ω resistive load. The load was placed in series on the output terminal and ran continuously for approximately 10 minutes to monitor the thermal dissipation and stability under extended operation. Finally, reliability under dynamic conditions was evaluated by rapidly toggling the control input to assess the TLP3547''s ability to switch on and off repeatedly with consistent timing, minimal delay variation, and without any observable degradation in conductivity performance.

For current monitoring, the Hall-Effect sensor was first evaluated under no load, being supplied with 5V to confirm idle voltage to be VCC/2. Following this a 9V battery was used to drive direct current across a 100KΩ potentiometer to measure the sensor's analog voltage output both in positive and negative current polarity. To evaluate the performance under an AC signal, the simulation transformer was applied in tandem with an 18Ω resistive load to both confirm whether the sensor captures values frequently enough to supply accurate measurements to the ESP32 and whether the sensor's output analog sensor waveform remained centered around the 0A midpoint. When using a DMM to measure the DC voltage, the output remained centered around this midpoint as expected. When switching to AC measurement, it showed the expected RMS voltage swing in relation to the AC current being drawn from the load. The sensor was tested at varying alternating current values to determine its accuracy in relation to known measurements taken with a DMM.

$$\varepsilon_x = \frac{1}{N}\sum_{i=1}^{N}|x_0 - x_i| \quad (5)$$

Using (67), we were able to determine the average absolute error from the target value. The results of said testing can be seen below.

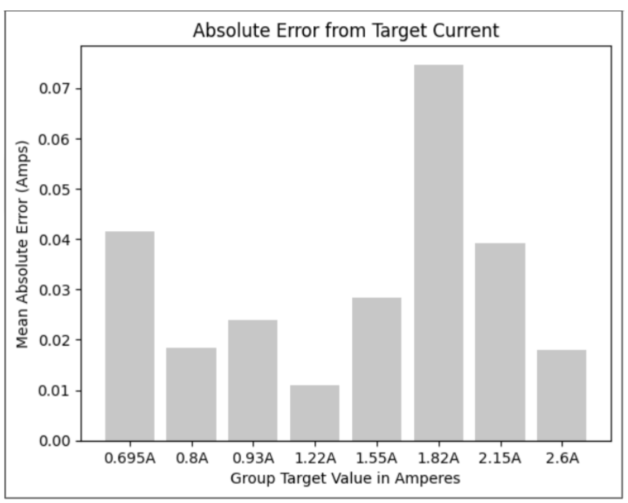

Fig. 6. Average Absolute Error for a known sample selection with known amperage.

Fig. 6 demonstrates that based on these preliminary assessments, the average deviation from the known target current was found to around 50 mA.

Initial testing of the embedded systems performance involved manual tests and writing small programs to interact with the ESP32. Once individual tested the full circuit was then tested all components were powered on from the buck regulator to ensure that each part was adequately powered and maintaining desired operational conditions. This included probing with a DMM to measure the voltage levels of nodes such as the input and outputs of the Hall-Effect sensor, and the output from the 3.3V linear regulator. Once proper operating voltages were confirmed, a load was applied across the breaker. Current measurements were taken across a 12 Ω, 18 Ω, and 24 Ω load. During this period of testing, evaluations were performed on the reported accuracy of a known 1.3A current draw, compared to the DMM, in relation to certain parameters for calculations being adjusted. To determine the sampling frequency needed capture necessary information to produce a meaningful RMS value, it was decided to follow the Nyquist Theorem

$$f_s > 2 \cdot f_{signal} \quad (6).$$

Which states that to capture meaningful information, the sampling frequency needs to be twice that of the incoming signal frequency. Since the American electrical grid operates at 60 Hz, it is penitent that the sampling frequency is greater than 120 Hz. The ESP32's high clock frequency makes performing this sampling trivially easy. Using (4), the RMS of the sinusoidal waveform was accurately captured, and then converted using the provided gain ratio in the ACS712-20A data sheet. Based on the current configuration of taking 100 samples along a single cycle at 6 KHz + the worst case SSR turn off time of 1.0ms, it's estimated that the average toggle time is roughly 8.2 ms.

VII. Conclusion

The S.A.B.R.E. project successfully demonstrates a modern, IoT-enabled alternative to conventional residential circuit breakers. By integrating a solid-state relay and an ESP32 microcontroller, the system provides highly responsive, real-time power monitoring and remote-control capabilities through a custom web application. Testing validated that the 24V/5A prototype operates safely within IEEE and IPC standards, achieving a rapid average trip response time of 8.2 ms and highly accurate current measurements. Ultimately, S.A.B.R.E. serves as a robust proof-of-concept, laying the groundwork for a full-scale implementation that offers homeowners unprecedented visibility and control over their residential energy consumption.

VIII. Biography

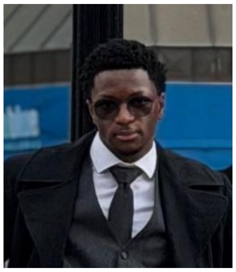

David Durosinmi is a 20-year-old graduating Computer Engineering student. David's career goals are to work for a large company such as AMD, NVIDIA, or Intel. Research and development keep David focused and interested in pursuing his dreams in computer development. His experience in software and web design was pivotal to the development of the SABRE smart breaker.

Carter Harman is a 22-year-old Computer Engineering student. Carter has taken a position with Advanced Micro Devices (AMD) as a Design Verification Engineer specializing in Verilog verification processes. Carter's experience in software and hardware development was the heart behind the circuitry, the firmware within the ESP32, and the backend of the SABRE smart breaker website.

Eliezer Urdaneta is a 23-year-old graduating Electrical Engineering student in the power and renewable energy track. Eliezer is seeking a career focused on substation protections and controls, working for a company such as HDR, KUA or OUC.

Emmanuel Lopez is a 23-year-old Electrical Engineering student. Emmanuel has taken a position with Quanta Infrastructure Solutions Group (QISG) as a Design Engineer specializing in substation design. Emmanuels experience in Computer-Aided Design (CAD) and hardware design was influential in designing the topology of the Printed Circuit Boards (PCBs) as well as the chassis to house the PCBs for the final demonstration.

Acknowledgement

The authors wish to acknowledge the assistance and support of Dr. Qun Zhou Sun, Professor Saleem Sahawneh, and Dr. Arthur Weeks.

References

[1] Espressif Systems, "ESP32-WROOM-32E & ESP32-WROOM-32UE Datasheet," Espressif Systems, Shanghai, China, pp. 1–50, 2023.

[2] Toshiba Electronic Devices & Storage Corp., "TLP3547 photorelay (MOSFET output) datasheet," Toshiba Semiconductor, pp. 1–20, Mar. 2020.

[3] Allegro MicroSystems, "Allegro Hall-Effect sensor ICs," Allegro MicroSystems, Manchester, NH, USA, pp. 1—–, 2013.

[4] Allegro MicroSystems, "ACS712 fully integrated, Hall-effect-based linear current sensor IC with 2.4 kVRMS isolation and a low-resistance current conductor," Allegro MicroSystems, Manchester, NH, USA, pp. 1–15, Feb. 2024.

[5] Microchip Technology Inc., "MCP970X family data sheet: low-power linear active thermistor ICs," Microchip Technology Inc., Chandler, AZ, USA, pp. 1–26, Feb. 2024.

[6] Electronics Tutorials, "RMS voltage of a sinusoidal AC waveform," Electronics-Tutorials.ws, pp. 1.

[7] European Agency for Safety and Health at Work, "Electricity – OSHwiki," OSHwiki, accessed Nov. 17, 2025. [Online]. Available: https://oshwiki.osha.europa.eu/en/themes/electricity

[8] IEEE Std C37.17-2022, IEEE Standard for Trip Systems for Low-Voltage Circuit Breakers, Institute of Electrical and Electronics Engineers, 2022.

[9] EPCI – Passive Components. Transformer Safety: IEC 61558 Standard. 7 Nov 2025 [accessed 2025 Nov 12]. https://passive-components.eu/transformer-safety-standards/

[10] IPC-2221A: Generic Standard on Printed Board Design. May 2003 [accessed 2025 Nov 12]. https://www-eng.lbl.gov/~shuman/NEXT/CURRENT_DESIGN/TP/MATERIALS/IPC-2221A(L).pdf